Supplement

The National Network Genomic Medicine Lung Cancer Germany (nNGM)

The National Network Genomic Medicine (nNGM) is a nationwide consortium comprising 31 certified oncology centers and more than 600 affiliated partner institutions across hospital and outpatient settings. The network provides standardized molecular diagnostic workflows, centralized interdisciplinary case evaluation, and structured reporting procedures. A dedicated digital platform (DigiNet) enables harmonized data transfer and integration between participating sites. Approximately 23,000 patients with lung cancer are managed within the network each year. Reimbursement agreements with statutory health insurers allow the majority of insured patients to access nNGM services. Recently, independent evaluations have shown that patients treated within nNGM experience superior survival outcomes compared with routine care [1].

Propensity Score Matching (PSM)

PSM was performed as an additional sensitivity analysis to minimize potential confounding due to imbalances in selected baseline characteristics and RECIST response categories. The propensity score (PS) was estimated using a logistic regression model including age at treatment initiation, sex, ECOG performance status, smoking history, histology, PD-L1 tumor proportion score, UICC stage, local tumor treatment and RECIST-based response category. The Hosmer–Lemeshow goodness-of-fit test indicated an adequate model fit and good calibration between observed and predicted values ($\chi^2(8) = 9.12$, $p = 0.332$). Matching was conducted in a 1:2 ratio using nearest-neighbor matching without replacement and a caliper width of 0.2 standard deviations of the logit of the PS. Covariate balance was assessed using standardized mean differences (SMD), with absolute values <0.2 considered negligible [2, 3]. After matching, all baseline covariates demonstrated adequate balance, confirming robustness of the matched cohorts.

Mutation analysis and determination of tumor mutation burden

FFPE tumor sections were deparaffinized and macrodissected. DNA was extracted using the Maxwell® RSC DNA FFPE kit on a Maxwell RSC 48 (Promega, Madison, WI, USA) according to the manufacturer's protocol. Hybrid capture–based comprehensive genomic profiling was performed with the SureSelect Cancer CGP Assay (Agilent, Santa Clara, CA, USA) and sequencing libraries prepared on a Magnis NGS Prep System (Agilent) according to manufacturer's specifications. Sequencing

was conducted on a NovaSeq X Plus (Illumina, San Diego, CA, USA) with a resulting sequence coverage of >100x. NGS data were analyzed on the DRAGEN Bio-IT platform (Illumina), considering variants with allele frequency ≥3%. Non-coding, intragenic, and intronic variants, as well as non-pathogenic genetic variants that are common in the population and currently have no known clinical significance (population frequency >0.1%), were excluded.

Tumor mutational burden (TMB) was calculated as previously described [4], including all synonymous and non-synonymous somatic variants (allele frequency >3%) and excluding variants present in dbSNP/gnomAD or recurrent drivers defined as >100 COSMIC entries.

Spatial single-cell gene expression profiling

Tissue sections of 5 µm thickness were cut from FFPE blocks and mounted onto the target area of Xenium glass slides. Slides were processed on the Xenium Analyzer (10x Genomics) according to the manufacturer's protocol using the Xenium Human Lung Gene Expression Panel supplemented with 50 custom add-on genes. Data preprocessing was performed on the instrument with the integrated Xenium analysis software. Transcripts were assigned to individual cells using nuclei-derived masks, rather than approximated cell boundaries, to minimize transcript bleed in densely packed regions. Assignment was conducted in Python based on 10x Genomics segmentation. Transcripts with Q-scores < 20 were excluded. Tumor regions were manually annotated in QuPath on H&E-stained whole-slide images from the same slides used for Xenium profiling. These images and annotations were registered to the Xenium Coordinate Space by alignment with the corresponding DAPI channel using the warpy workflow [5]. Downstream analyses were restricted to cells within annotated tumor regions, excluding adjacent non-malignant tissue. All analyses were performed in R (version 4.2.2) using the Seurat package (version 5.1.0). In short, single-cell transcriptomes were normalized by SCTransform, integrated by RPCA, and clustered. Cell types were annotated cluster-wise based on expression of canonical cell type marker genes. For further details see analysis code provided under https://doi.org/10.5281/zenodo.17818852.

Quantification of tumor-infiltrating lymphocytes

Paraffin-embedded tissue samples were sectioned at a thickness of 2-3 µm and stained with hematoxylin and eosin (H&E) for standard histopathological evaluation.

The slides were digitized using a PANNORAMIC 1000 scanner (3DHISTECH, Budapest, Hungary) and examined with the open-source platform QuPath (version 0.3.2) [6]. Cell detection was carried out based on optical density sums, otherwise applying default parameters. A pathologist (P.B.) manually annotated tumor regions as well as representative examples of lymphocytes and non-lymphocyte cells. To adjust for inter-slide staining differences, a separate Random Forest Classifier was trained for each case to categorize cells into lymphocytes versus other cell types. Lymphocyte counts and tumor area, were then extracted from QuPath.

Additional Literature

1. Kastner A, Kron A, van den Berg N *et al.*, Evaluation of the effectiveness of a nationwide precision medicine program for patients with advanced non-small cell lung cancer in Germany: a historical cohort analysis. Lancet Reg Health Eur, 2024. 36: p. 100788.

2. Rubin DB, Estimating causal effects from large data sets using propensity scores. Ann Intern Med, 1997. 127(8 Pt 2): p. 757-63.

3. Stuart EA, Matching methods for causal inference: A review and a look forward. Stat Sci, 2010. 25(1): p. 1-21.

4. Chalmers ZR, Connelly CF, Fabrizio D *et al.*, Analysis of 100,000 human cancer genomes reveals the landscape of tumor mutational burden. Genome Med, 2017. 9(1): p. 34.

5. Chiaruttini N, Burri O, Haub P *et al.*, An Open-Source Whole Slide Image Registration Workflow at Cellular Precision Using Fiji, QuPath and Elastix. Frontiers in Computer Science, 2022. Volume 3 - 2021.

6. Bankhead P, Loughrey MB, Fernandez JA *et al.*, QuPath: Open source software for digital pathology image analysis. Sci Rep, 2017. 7(1): p. 16878.

Figure legends

Figure S1 – Objective response rate (ORR) in cohort B. Shown are best overall responses to ICB according to RECIST. “X” denotes patients with progressive disease.

Figure S2 – Time to PET/CT (A) and distribution of PET avidities in non-CMR patients and outcome of the respective biopsies (B). Among the 126 patients in cohort A, the median time to PET/CT was 25.6 mo. [25.1–26.9] (A), 48 (38%) showed a non-complete metabolic response (non-CMR). Distribution of PET-avid lesions was as follows (B): 22 (46%) at the primary tumor site with viable cancer confirmed in 6 cases (27%), 13 (27%) in lymph nodes with cancer in 3 cases (23%), 4 (8%) in metastatic sites with cancer in 3 cases (75%), 8 (17%) as new lesions with cancer in 6 cases (75%), and 1 (2%) not further specified and not biopsied. Notably, lymph node avidities showed the highest false-positive rate, with cancer excluded in 77% of re-biopsied cases.

Figure S3 – Time to onset, grading, and organ system distribution of ICB-limiting irAEs. Median time to irAE was 31.6 months [27.9 – 33.4] (A). A total of 60 patients experienced an ICB-limiting irAE, including 4 in cohort A and 56 in cohort B. While most irAEs were low-grade (G1–2; 64%), one third (36%) led to treatment discontinuation due to high-grade toxicity (G3–4), including one G4 event attributed to ICB-mediated non-inflammatory left-ventricular dysfunction (B; left y axis: percentage of irAE grades, right y axis: no. of patients affected).

Figure S4 – Sensitivity Analysis of OS (Propensity Score Matching)

Figure S5 – OS in cohort A by PET policy (systematic vs. individualized, A), by institutional type (academic vs. community-based hospitals, B) and by PET/CT outcomes and re-biopsy (C)

Figure S6 – Lung cancer specific OS (A) and OS2 (B) in patients having received subsequent treatment(s) following disease progression

Figure S7 – Progression-free Survival. (A) Dynamic Kaplan-Meier Plot for PFS in both cohorts. (B) Forest Plot displaying various subgroups (patient-related, tumor-related)

Figure S8 – Cox proportional hazard regression for OS (A) and PFS (B)

Figure S9 – Second malignancies in both cohorts. (A) Among patients in cohort A (n=126), 13/126 (10%) developed a second cancer, including 10/126 (8%) second primary lung cancers (SPLC) and 3/126 (2%) other malignancies. In cohort B (n=329), 13/329 (4%) developed a second cancer, including 8/329 (2%) SPLC and 5/329 (2%) other malignancies. (B) In both cohorts, the majority of secondary malignancies were amenable to local ablative treatment (LAT, i.e. surgery or SBRT). In cohort A, LAT was performed in 7 SPLC (70%) and 2 other malignancies (67%), while in cohort B, 5 SPLC (63%) and 3 other malignancies (60%) received LAT.

Figure S10 – Mutational profiling of lung cancers before and after ICB. (A+B) Adequate DNA quantity and quality for mutational analysis before (T1) and after (T2) ICB therapy were obtained from 31 cases. (A) Tumors with progressive or persistent

primary tumors displayed similar mutational profiles. (B) Second primary lung cancers exhibited divergent mutational profiles compared to the initial primary tumors.

Figure S11 – Clinical metadata and quality control parameters of spatial transcriptomic profiling of lung cancers before and after ICB. (A) Clinical metadata and quality control parameters per tissue sample. (B) Expression of main cell type markers per cell type. (C) Correlation of histological TIL densities with both lymphocyte fractions ($CD4^+$ T, $CD8^+$ T, and B cells) and the abundance of immune-rich niches derived from spatial transcriptomics. (D). Spatial maps per tissue sample, color-coded by cell type.

Table S12 – Baseline characteristics in the sensitivity cohort analysis (Propensity Score Matching)

Table S13 – Distribution of disease progression patterns (A) and subsequent treatments (B) in all patients and by cohort

Figure S1 – Objective response rate (ORR) in cohort B
Shown are best overall responses to ICB according to RECIST

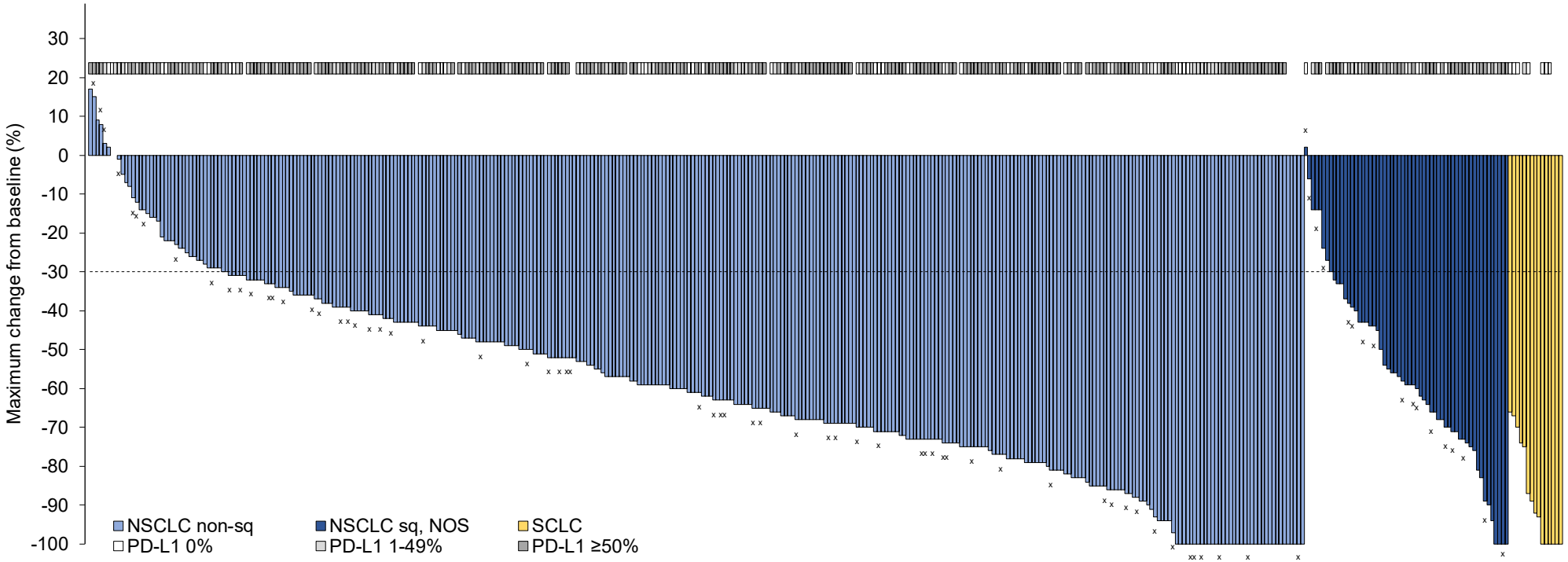

Figure S2 – Time to PET/CT (A) and distribution of PET avidities in non-CMR patients and outcome of the respective biopsies (B)

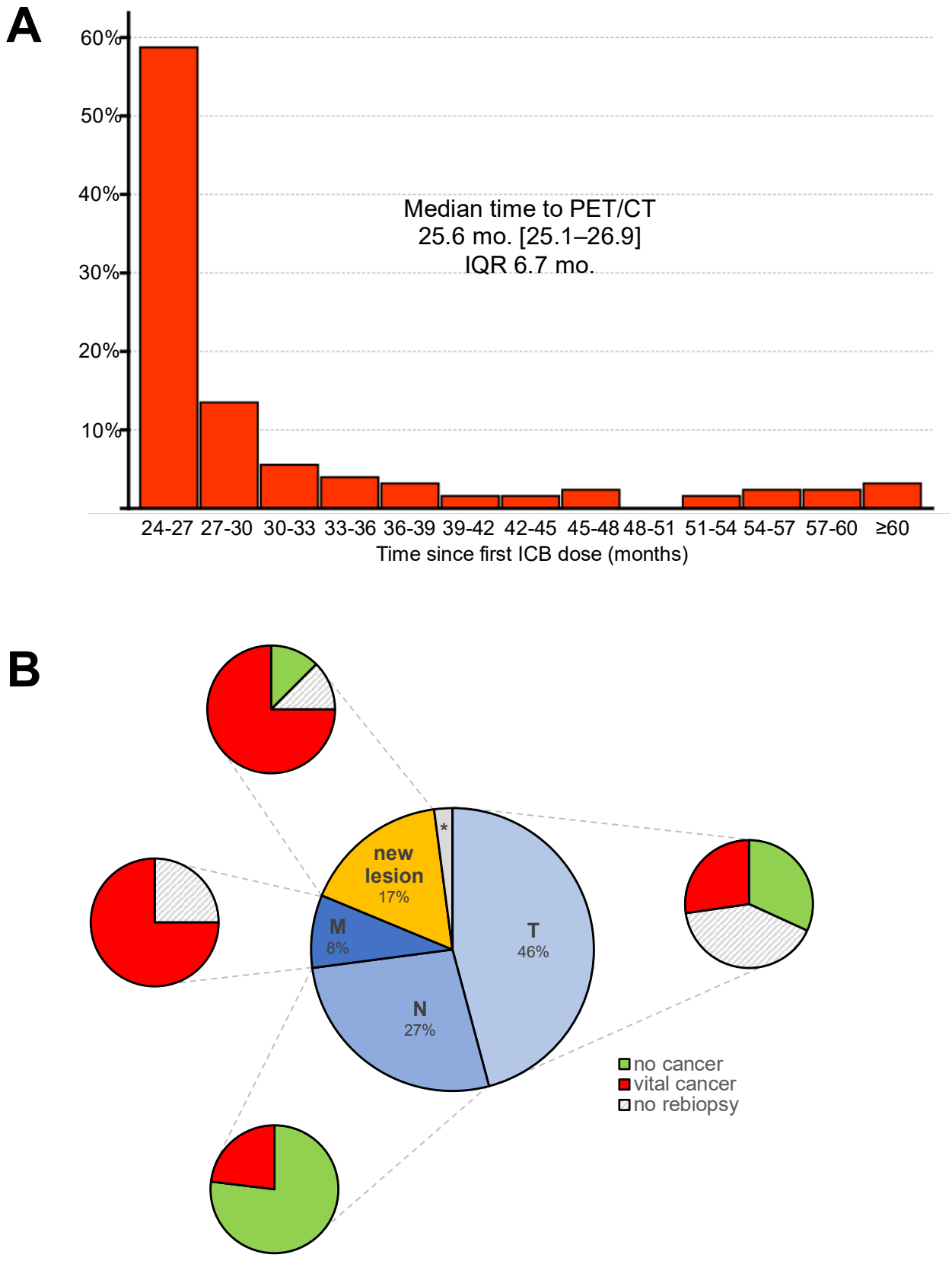

Abbreviations: ICB: immune-checkpoint blockade, T: primary tumor site, N: lymph node(s), M: metastatic site, *: site not reported

Figure S3 – Time to onset (A), grading, and organ system distribution of ICB-limiting irAEs (B)

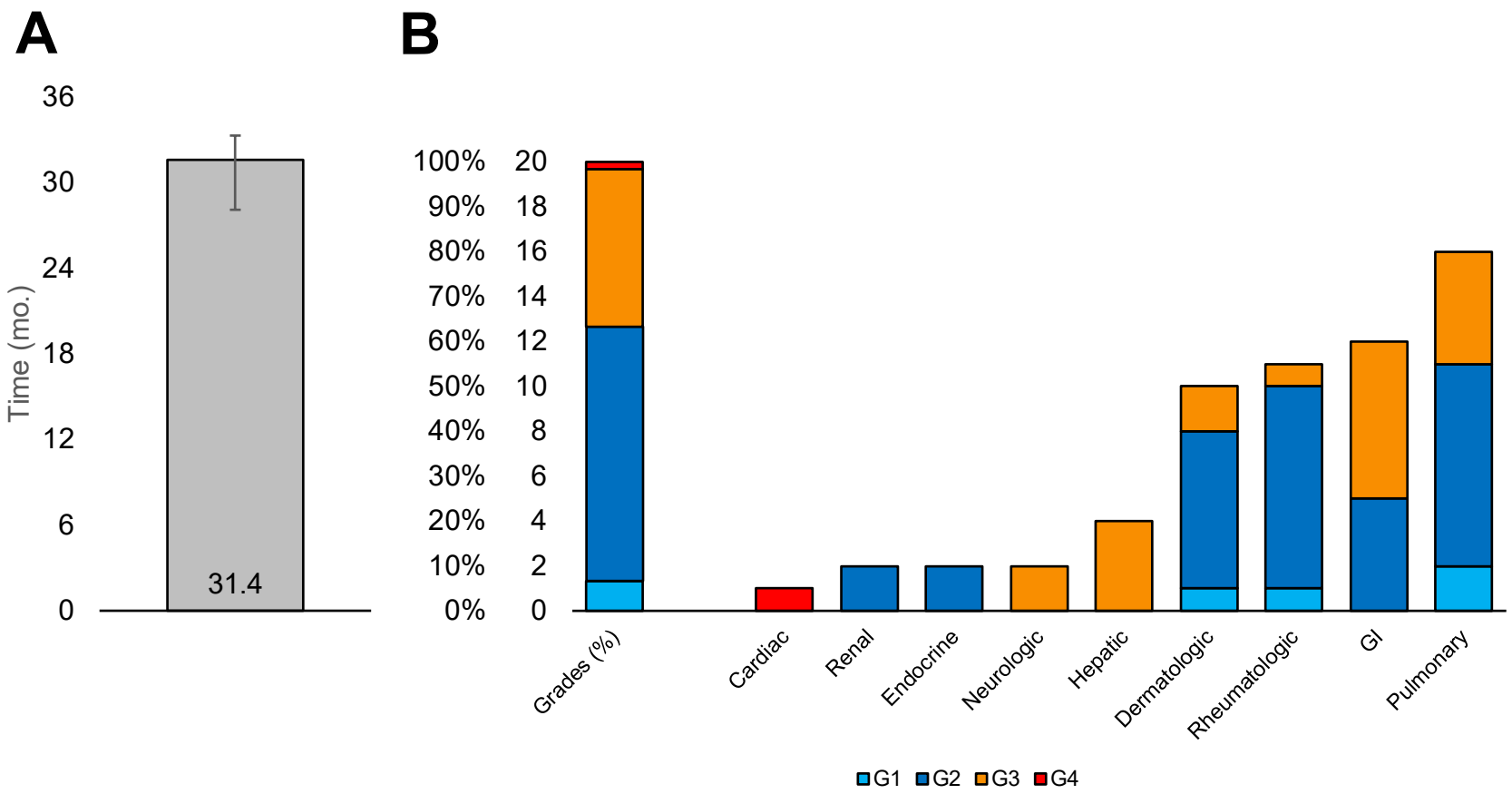

Cardiac toxicity:	non-inflammatory left ventricular dysfunction (NILVD)
Renal toxicity:	nephritis
Endocrinopathies:	adrenal insufficiency, type 1 diabetes mellitus
Neurological toxicity:	encephalitis
Hepatotoxicity:	hepatitis
Skin toxicity:	bullous dermatitis, neutrophilic dermatosis, rash
Rheumatological toxicity:	inflammatory arthritis, myositis, psoriasis
Gastrointestinal toxicity:	colitis, lymphocytic gastritis, pancreatitis
Pulmonary toxicity:	pneumonitis

Figure S4 – Sensitivity Analysis of OS (Propensity Score Matching)

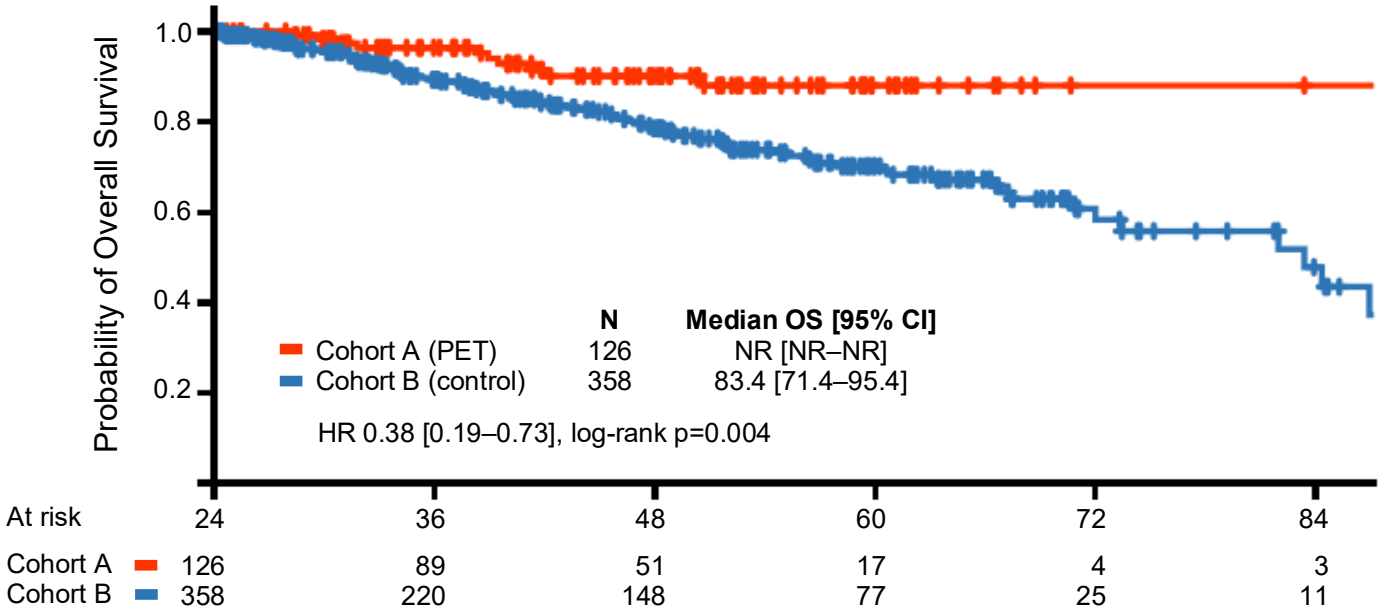

Figure S5 – OS in cohort A by PET policy (systematic vs. individualized, A), by institutional type (academic vs. community-based hospitals, B) and by PET/CT outcomes and re-biopsy (C)

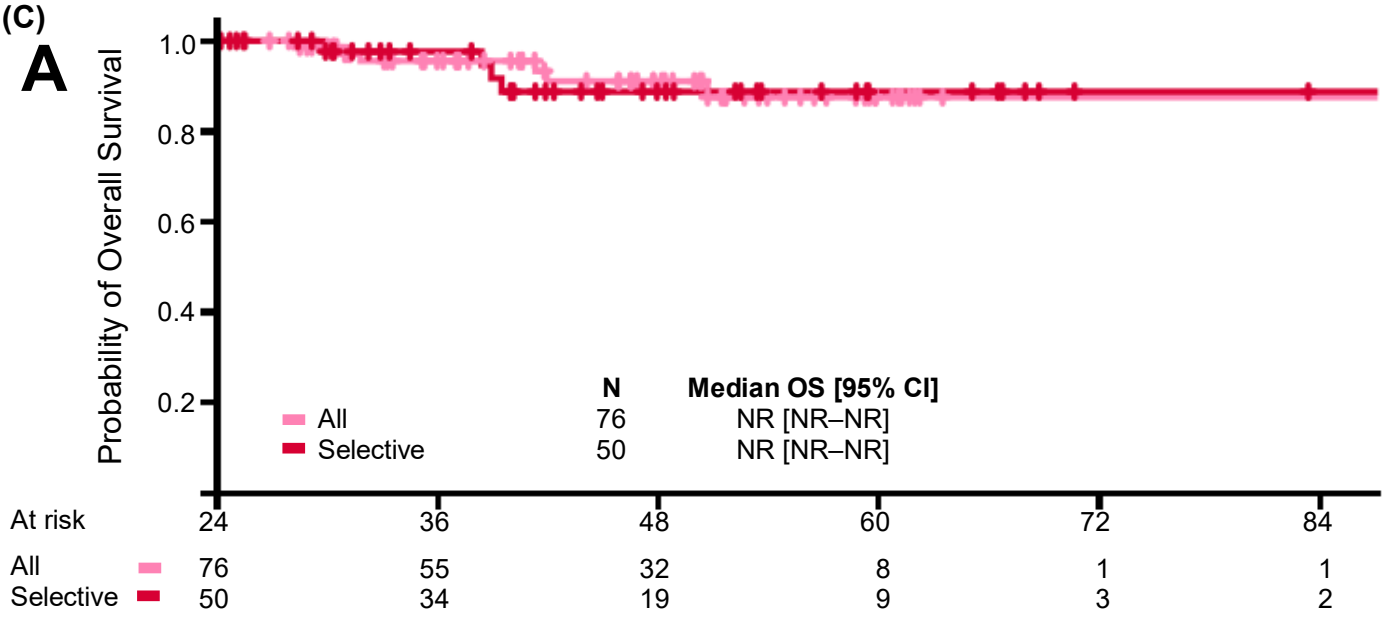

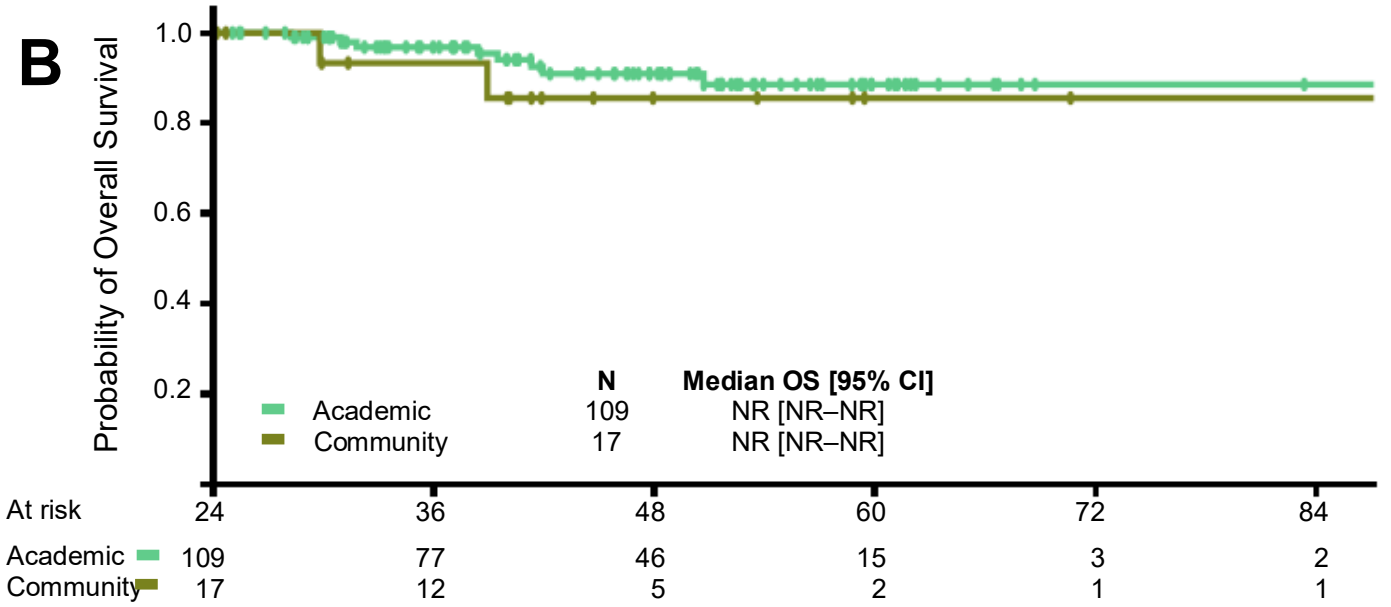

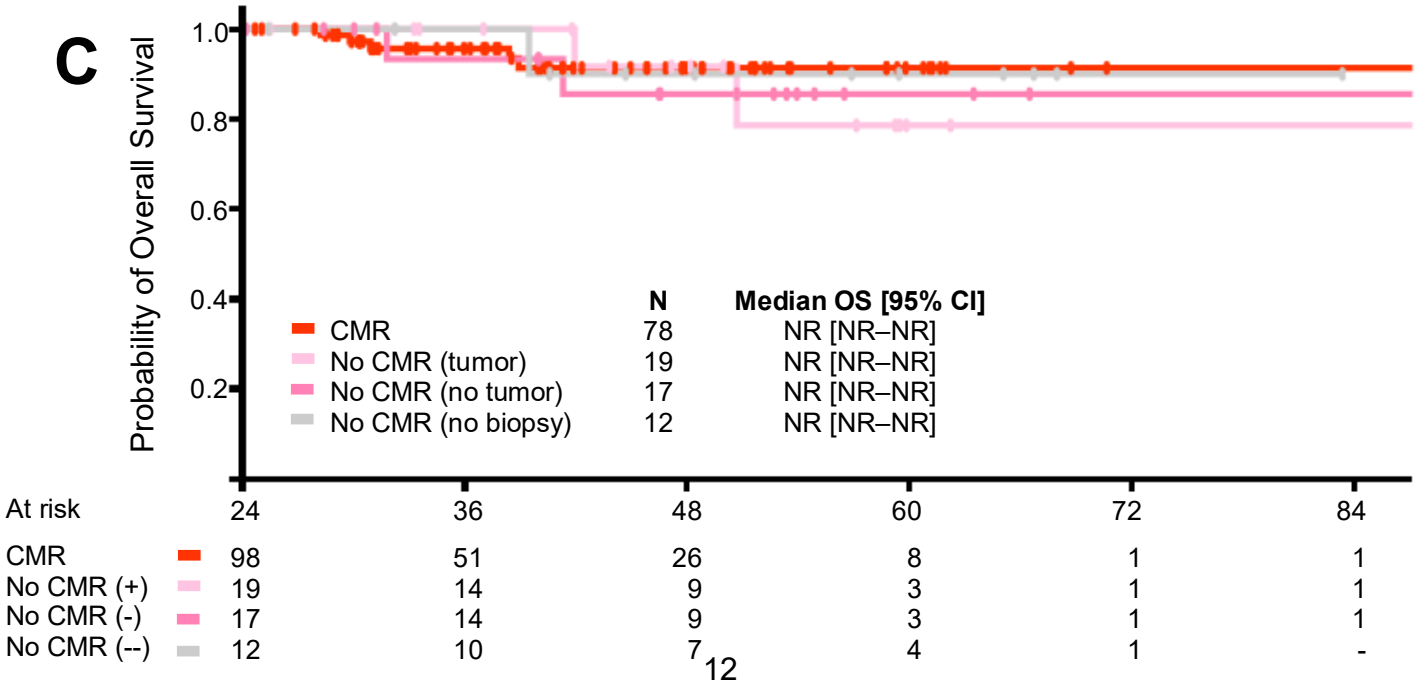

Figure S6 – Lung cancer specific OS (A) and OS2 (B) in patients having received subsequent treatment(s) following disease progression

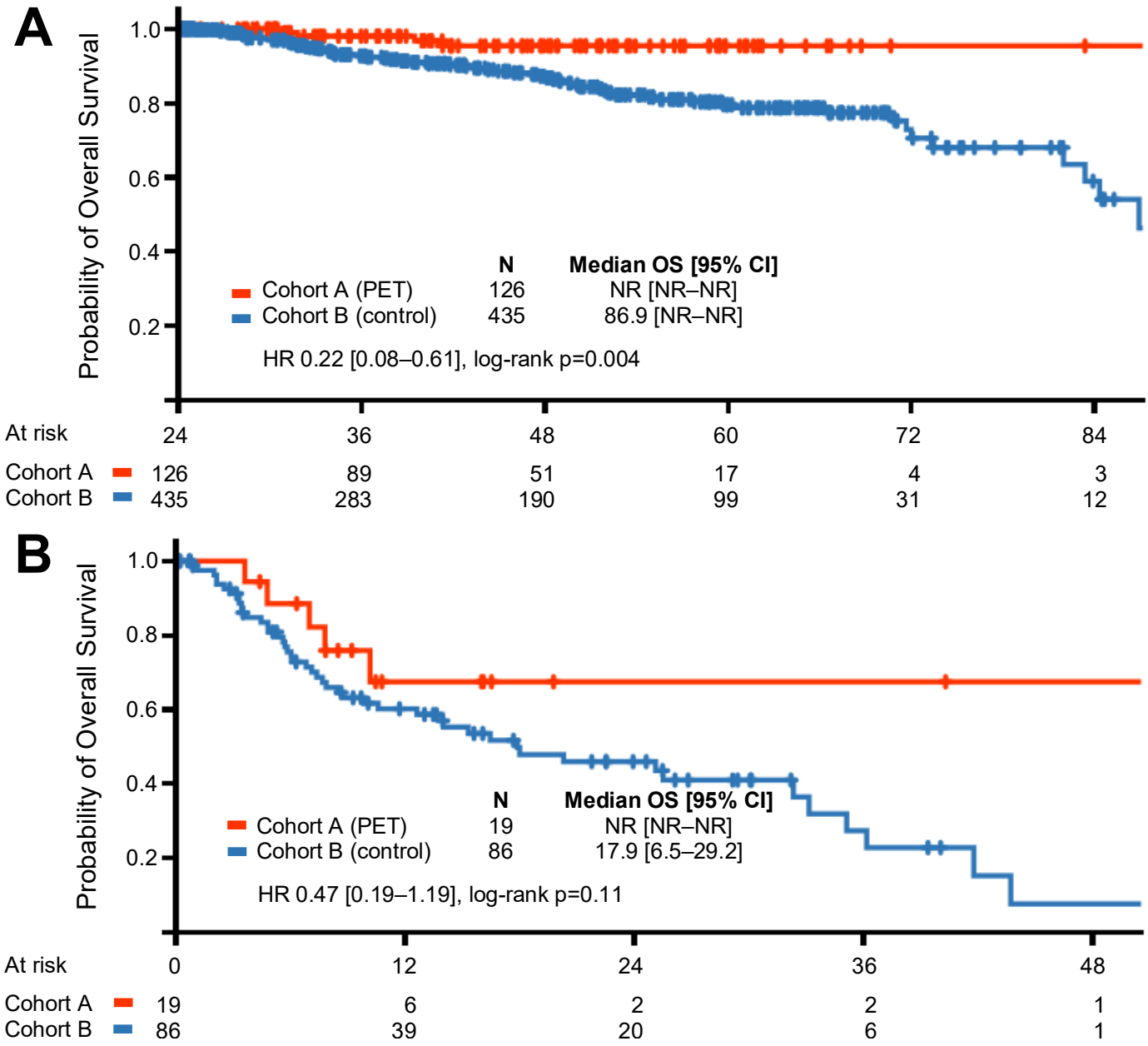

Figure S7 – Progression-free Survival. (A) Dynamic Kaplan-Meier Plot for PFS in both cohorts. (B) Forest Plot displaying various subgroups (patient-related, tumor-related).

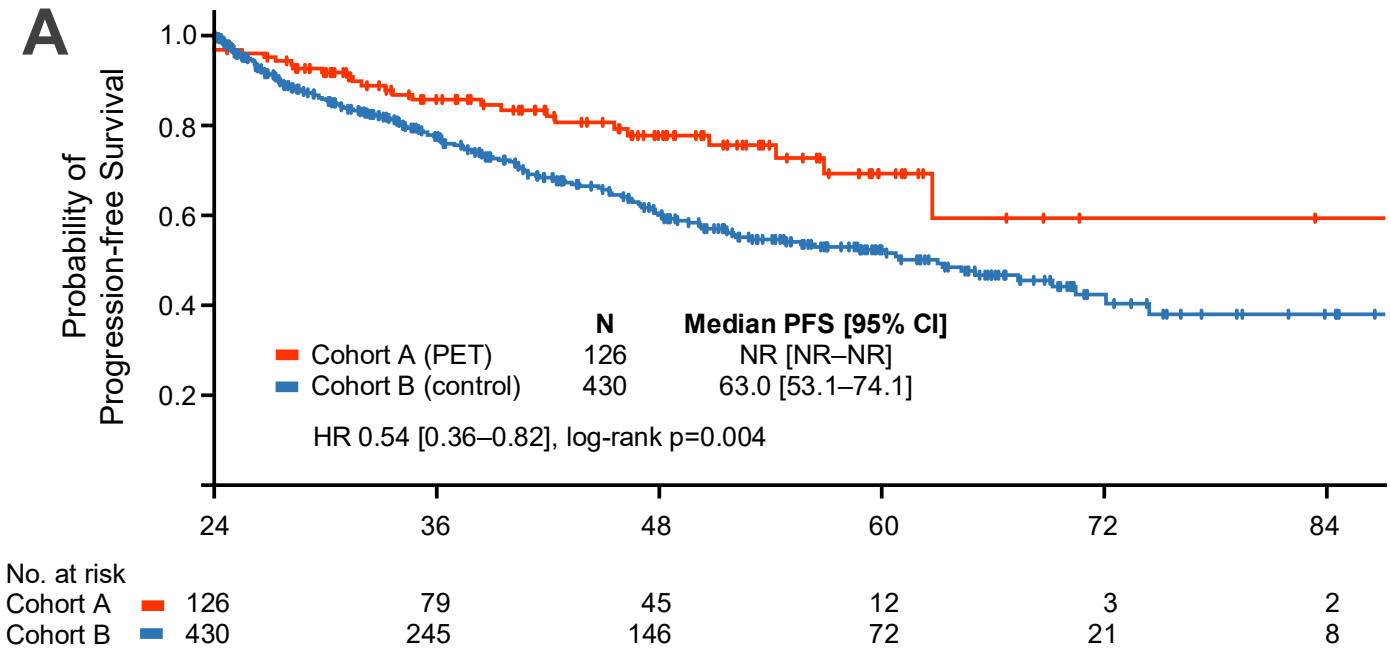

B

	HR	[95% CI]	p-value	n	events
PFS					
Cohort A vs. B	**0.55**	**[0.35–0.87]**	**0.01***	455	166
Age					
≤65	0.69	[0.37–1.29]	0.25	237	82
>65	0.44	[0.23–0.86]	0.02*	218	84
Sex					
Female	0.45	[0.21–0.94]	0.03*	206	66
Male	0.64	[0.36–1.14]	0.13	249	100
ECOG					
0	0.67	[0.32–1.41]	0.53	199	61
1	0.50	[0.27–0.94]	0.03*	209	80
≥2	0.51	[0.11–2.26]	0.37	36	17
Histology					
non-sq NSCLC	0.61	[0.35–1.05]	0.08	324	119
sq-NSCLC/NOS	0.49	[0.20–1.18]	0.11	94	36
SCLC	0.33	[0.04–2.73]	0.30	37	11
PD-L1 expression					
0%	0.53	[0.15–1.83]	0.32	56	21
1–49%	0.79	[0.32–1.95]	0.61	81	32
≥50%	0.47	[0.25–0.89]	0.02*	271	98
Unknown/SCLC	0.58	[0.13–2.66]	0.48		
Initial stage at start ICI					
IV	0.58	[0.36–0.95]	0.03*	383	138
III/recurrent	0.43	[0.13–1.44]	0.17	72	28
Brain metastases					
Yes	0.35	[0.11–1.14]	0.08	96	35
No	0.61	[0.38–1.00]	0.05*	359	131
Local treatment before/during ICB					
Yes	0.76	[0.37–1.56]	0.45	148	52
No	0.47	[0.26–0.86]	0.01*	307	114
Response (RECIST)					
PR/CR	0.61	[0.38–0.98]	0.04*	368	126
SD	0.32	[0.04–2.43]	0.27	44	20

Figure S8 – Cox proportional hazard regression for OS (A) and PFS (B; univariable left, multivariable right)

A

	HR	[95% CI]	p-value	HR	[95% CI]	p-value	n	events
OS								
Cohort A vs. B	**0.35**	**[0.18–0.68]**	**0.002***	**0.38**	**[0.20–0.74]**	**0.004***	455	105
Age								
≤65 vs. >65	0.55	[0.37–0.81]	0.002*	0.55	[0.37–0.83]	0.004*	455	105
Sex								
Female vs. Male	1.25	[0.85–1.85]	0.25	1.21	[0.81–1.80]	0.35	455	105
ECOG-PS								
0-1 (ref.)	1.00			1.00			408	87
≥2	1.34	[0.69–2.57]	0.39	1.11	[0.56–2.20]	0.76	36	26
Unknown	2.96	[1.43–6.11]	0.003*	2.19	[1.04–4.62]	0.04*	11	3
Histology								
non-sq NSCLC (ref.)	1.00			1.00			324	75
sq-NSCLC/NOS	1.35	[0.87–2.11]	0.18	1.35	[0.84–2.16]	0.21	94	26
SCLC	0.59	[0.22–1.62]	0.31	0.42	[0.09–1.93]	0.27	37	4
PD-L1 expression								
0% (ref.)	1.00			1.00			56	12
1–49%	1.07	[0.53–2.18]	0.85	1.28	[0.61–2.65]	0.51	81	21
≥50%	0.84	[0.45–1.57]	0.59	1.04	[0.55–1.97]	0.90	271	65
Unknown/SCLC	0.66	[0.26–1.67]	0.38	1.71	[0.47–6.22]	0.42	47	7
Initial stage at start ICI								
IV vs. III/recurrent	0.72	[0.45–1.17]	0.19	0.93	[0.55–1.55]	0.77	455	105
Brain metastases								
Yes vs. No	0.79	[0.48–1.30]	0.36	0.98	[0.57–1.69]	0.94	455	105
Local treatment before/during ICI								
Yes vs. No	1.00	[0.66–1.50]	0.99	1.20	[0.77–1.88]	0.42	455	105
Response (RECIST)								
PR/CR	1.00			1.00			368	76
SD	2.23	[1.32–3.78]	0.003*	2.23	[1.29–3.87]	0.004*	44	17
NE/NA	1.36	[0.74–2.50]	0.33	1.36	[0.72–2.58]	0.34	43	12

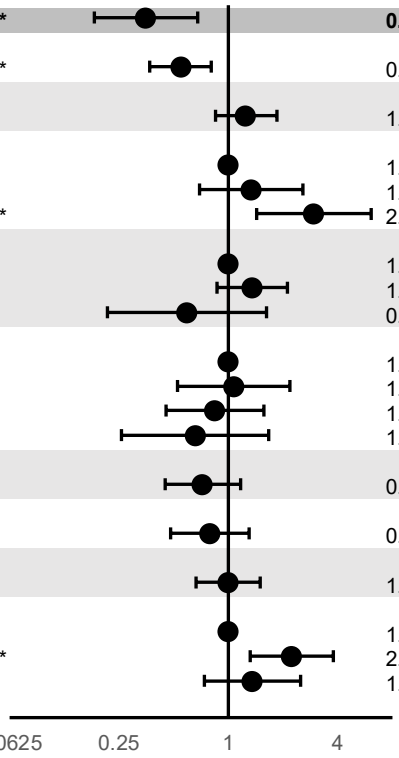

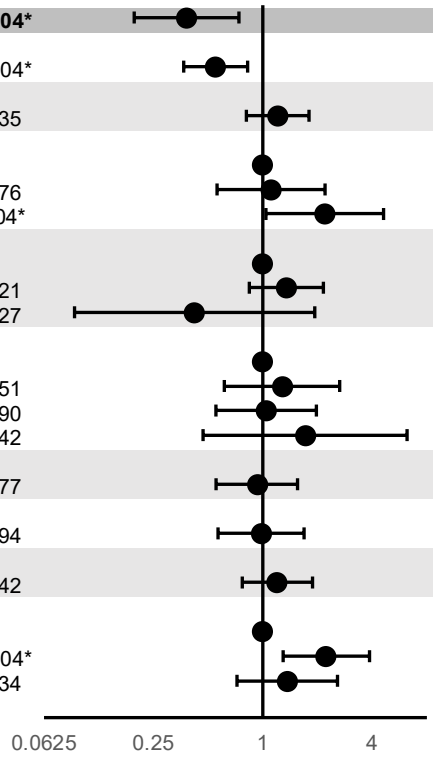

B

	HR	[95% CI]	p-value	HR	[95% CI]	p-value	n	events
PFS								
Cohort A vs. B	**0.55**	**[0.35–0.87]**	**0.01***	**0.58**	**[0.37–0.92]**	**0.02***	455	166
Age								
≤65 vs. >65	0.84	[0.62–1.14	0.26	0.85	[0.61–1.17]	0.31	455	166
Sex								
Female vs. Male	1.31	[0.96–1.78]	0.09	1.28	[0.93–1.75]	0.13	455	166
ECOG-PS								
0-1 (ref.)	1.00			1.00			408	141
≥2	1.43	[0.86–2.37]	0.16	1.4	[0.82–2.37]	0.22	36	17
Unknown	2.12	[1.04–4.33]	0.04*	1.83	[0.88–3.78]	0.10	11	8
Histology								
non-sq NSCLC (ref.)	1.00			1.00			324	119
sq-NSCLC/NOS	1.09	[0.75–1.58]	0.11	1.12	[0.76–1.66]	0.58	94	36
SCLC	0.94	[0.51–1.74]	0.84	0.81	[0.25–2.58]	0.72	37	11
PD-L1 expression								
0% (ref.)	1.00			1.00			56	21
1–49%	0.96	[0.56–1.67]	0.90	1.03	[0.59–1.81]	0.92	81	32
≥50%	0.73	[0.46–1.17]	0.19	0.75	[0.46–1.22]	0.25	271	98
Unknown/SCLC	0.78	[0.40–1.52]	0.47	1.07	[0.36–3.18]	0.91	47	15
Initial stage at start ICI								
IV vs. III/recurrent	0.88	[0.59–1.33]	0.55	0.98	[0.64–1.51]	0.93	455	166
Brain metastases								
Yes vs. No	1.02	[0.70–1.47]	0.94	1.18	[0.78–1.79]	0.43	455	166
Local treatment before/during ICI								
Yes vs. No	0.97	[0.70–1.34]	0.83	0.95	[0.67–1.36]	0.78	455	166
Response (RECIST)								
PR/CR (ref.)	1.00			1.00			368	126
SD	1.57	[0.98–2.52]	0.06	1.52	[0.93–2.48]	0.09	44	20
NE/NA	1.46	[0.91–2.34]	0.78	1.32	[0.81–2.16]	0.27	43	20

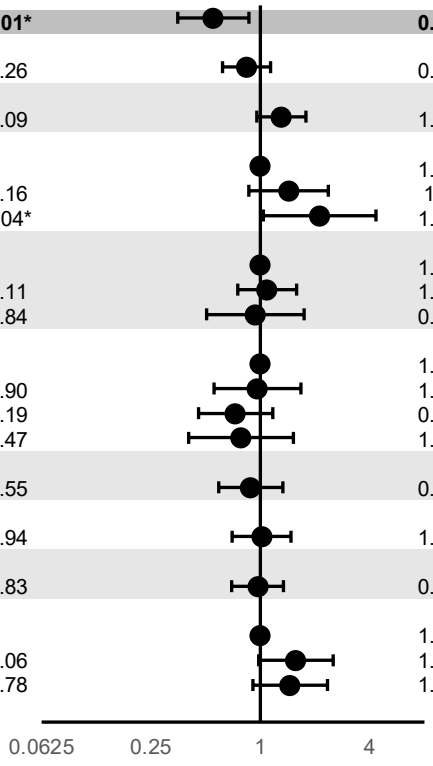

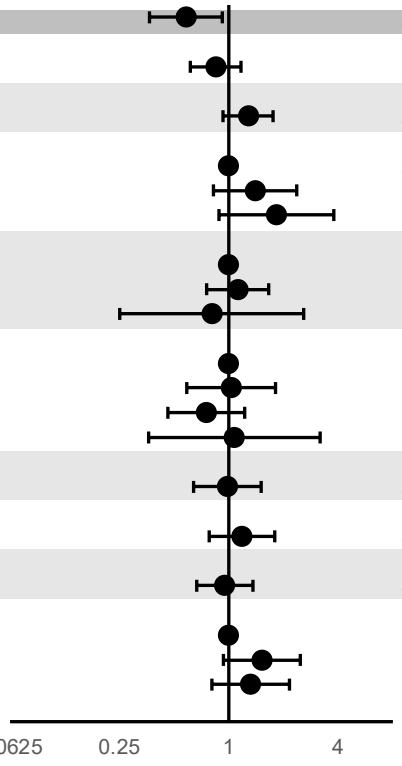

Figure S9 – Secondary malignancies in cohort A and B with distribution of entities (second primary lung cancer and others; A) and the respective treatments (B)

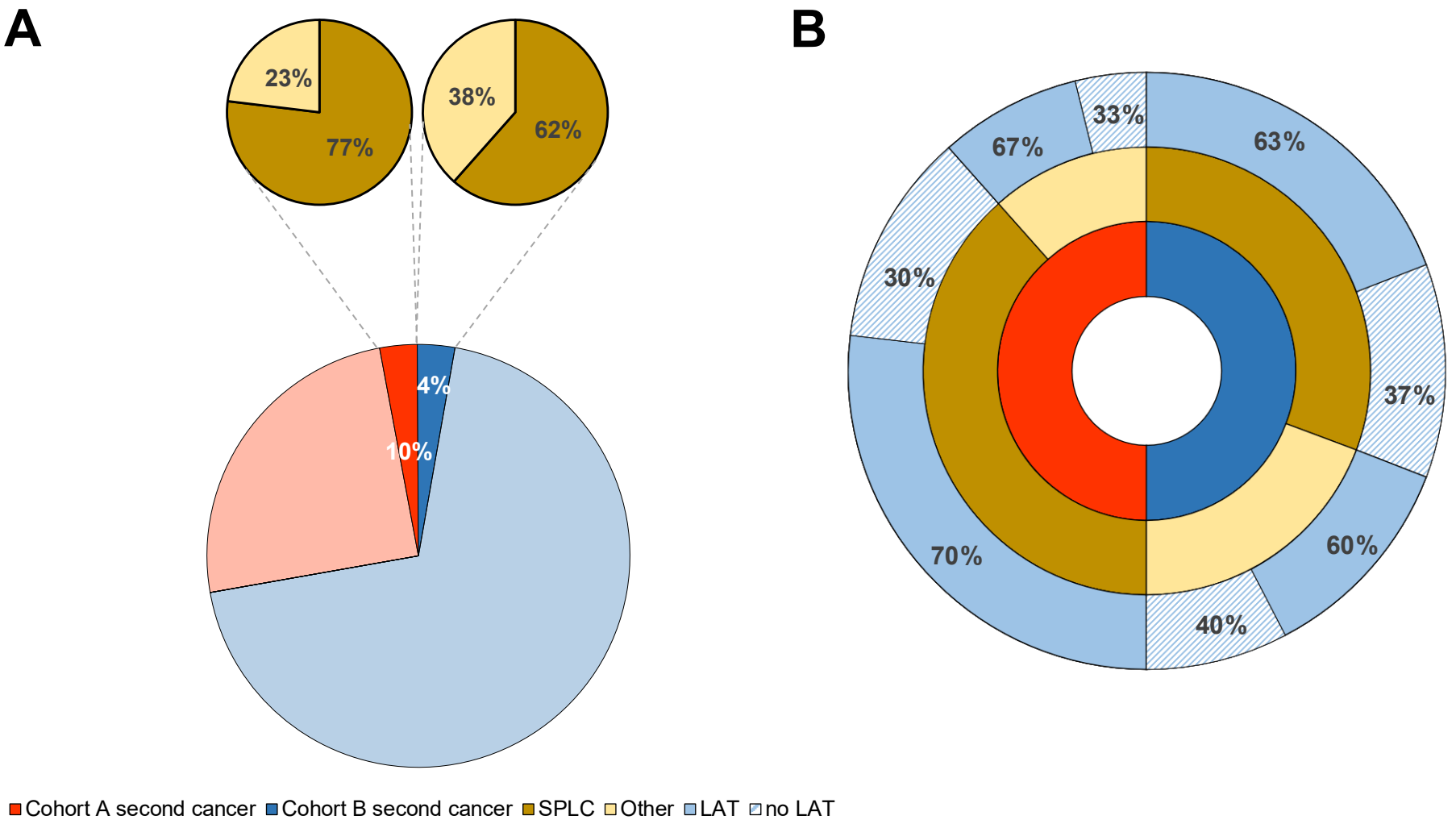

Abbreviations: SPLC, second primary lung cancer; LAT, local ablative treatment
Other: HNSCC n=2; BC n=2; CRC, myeloma, PDAC, sarcoma (each n=1)

Figure S10 – Mutational profiling of lung cancers before and after ICB

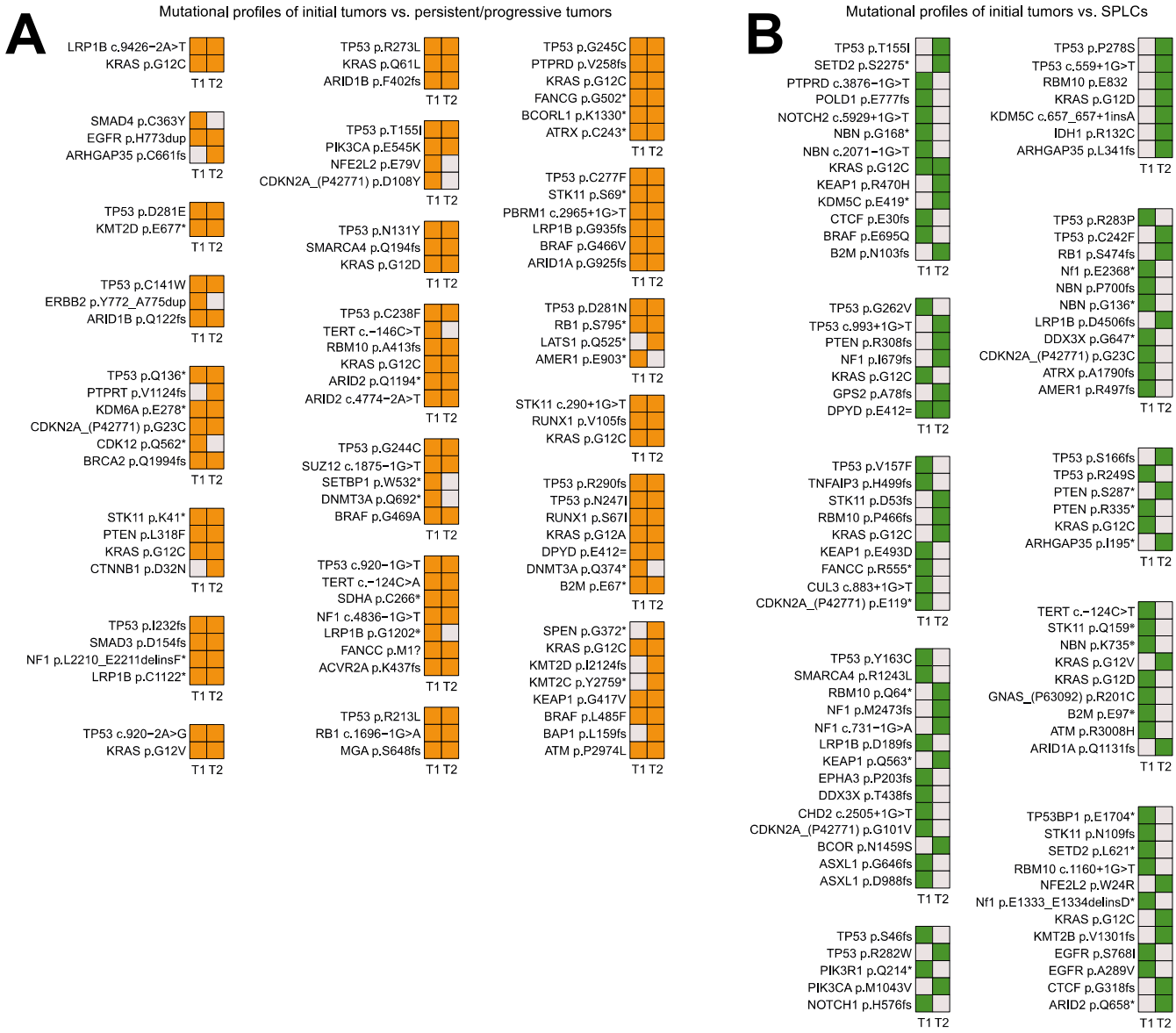

Figure S11 – Clinical metadata and quality control parameters of spatial transcriptomic profiling of lung cancers before and after ICB

A

Patient ID	Timepoint	Sampling site	Sampling type	Histology	Classification of second sample	Number of cells	Median number of transcripts	Median number of genes
p121	T1	Lung	Resection	ADC	-	163.208	53	34
p121	T2	Lung	Resection	ADC	SPLC	288.279	62	34
p122	T1	Lung	Biopsy	ADC	-	22.112	11	9
p122	T2	Lung	Biopsy	ADC	Persistence	78.154	38	27
p123	T1	Mouth	Biopsy	ADC	-	24.473	45	26
p123	T2	Lung	Biopsy	ADC	Persistence	6.595	58	39
p124	T2	Lung	Biopsy	SCLC	Progression	33.108	72	39
p125	T2	Lung	Biopsy	ADC	Persistence	29.736	32	22
p172	T1	Lung	Resection	ADC	-	125.399	28	18
p173	T1	Liver	Biopsy	ADC	-	3.815	55	33
p173	T2	Lung	Biopsy	ADC	Progression	36.345	49	29
p174	T1	Liver	Biopsy	ADC	-	21.131	38	23
p174	T2	Lymph node	Resection	ADC	Progression	11.088	111	46

B

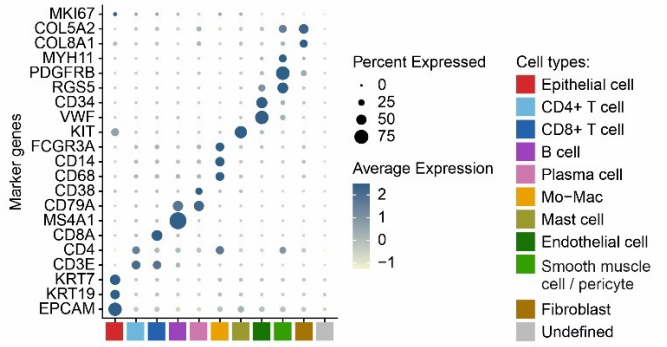

C

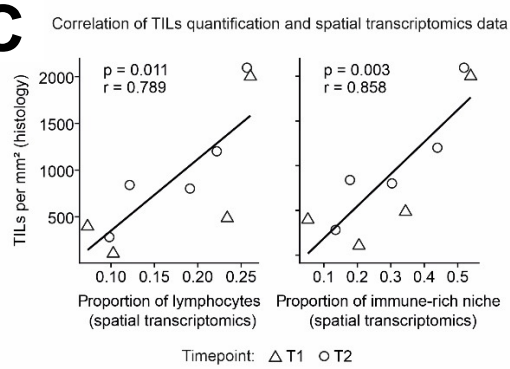

D

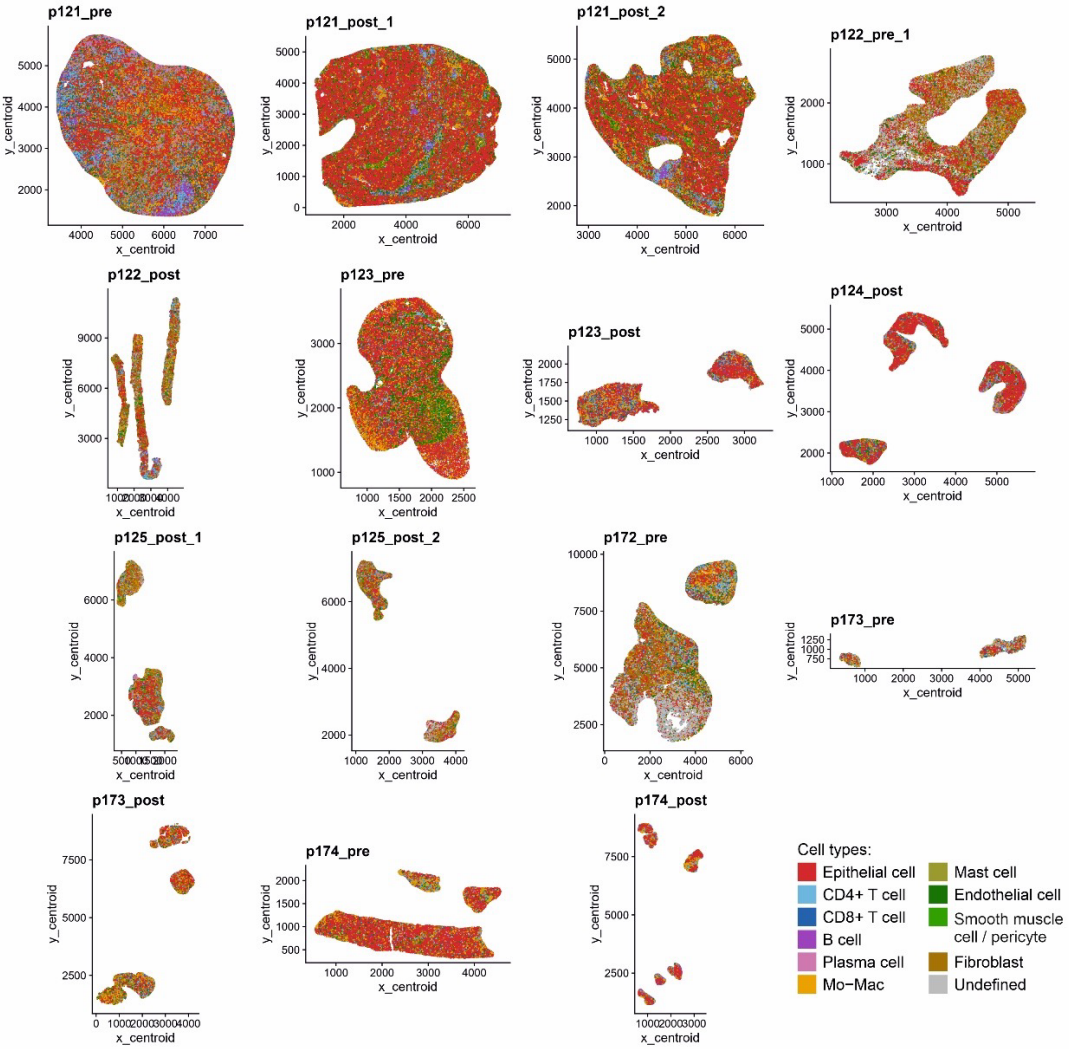

Table S12 – Baseline characteristics in the sensitivity cohort analysis (Propensity Score Matching)

Variable	PET (n=126)	control (n=252)	SMD	p-value
Age, median (range)	65 (34-83)	65 (35-86)	0.03	0.24
Sex			0.05	0.51
Female, n (%)	62 (49.2)	115 (45.6)		
Male, n (%)	64 (50.8)	137 (54.4)		
ECOG-PS			0.08	0.42
0, n (%)	50 (39.7)	118 (46.8)		
1, n (%)	67 (53.2)	118 (46.8)		
≥2, n (%)	9 (7.1)	16 (6.3)		
Smoking history			0.04	0.39
Never, n (%)	10 (7.9)	12 (4.8)		
Ever, n (%)	115 (91.3)	236 (93.7)		
Missing, n (%)	1 (91.3)	4 (1.6)		
Histology			0.14	0.18
non-squamous NSCLC, n (%)	79 (62.7)	180 (71.4)		
squamous/NOS NSCLC, n (%)	32 (25.4)	53 (21.0)		
SCLC, n (%)	15 (11.9)	19 (7.5)		
PD-L1 expression, median (95%CI)	70 (40-75))	70 (60-80)	0.08	0.96
0%, n (%)	23 (18.3)	34 (13.5)		
1-49%, n (%)	26 (20.6)	49 (19.4)		
≥50%, n (%)	68 (54.0)	153 (60.7)		
missing, n (%)	9 (7.1)	16 (6.3)		
Initial stage at start ICI			0.07	0.82
IVA, n (%)	38 (30.2)	82 (32.5)		
IVB, n (%)	65 (51.6)	133 (52.8)		
III n (%)	7 (5.6)	27 (10.7)		
recurrent, n (%)	16 (12.7)	10 (4.0)		
Brain metastases at start ICI			0.07	0.42
Y, n (%)	23 (18.3)	55 (21.8)		
N, n (%)	103 (81.7)	197 (78.2)		
First-line treatment			-0.07	0.38
ICB monotherapy, n (%)	56 (44.4)	124 (49.2)		
ICB + chemotherapy, n (%)	70 (55.6)	128 (50.8)		
Local treatment before/during ICI			-0.09	0.22
Y, n (%)	48 (38.1)	80 (31.7)		
N, n (%)	78 (61.9)	172 (68.3)		
RECIST				
ORR	95.1 (89.7-98.2)	93.4 (89.5-96.2)	-0.14	0.64
SD	6 (4.8)	16 (6.3)		
PR	98 (77.8)	200 (79.4)		
CR	19 (15.1)	26 (10.3)		
missing/NE	3 (2.4)	10 (4.0)		

Table S13 – Distribution of disease progression patterns (A) and subsequent treatments (B) in all patients and by cohort

A

Variable	All patients (N=124)	cohort A (N=19)	cohort B (N=105)	p-value
Distribution of disease progression patterns				0.37
Oligo-progression	88 (71.0)	15 (78.9)	73 (69.5)	
Thoracic (lung ± regional lymph nodes)	59 (47.6)	10 (52.6)	49 (46.7)	
Brain	15 (12.1)	3 (15.8)	12 (11.4)	
Other*	8 (6.5)	2 (10.5)	6 (5.7)	
Missing	6 (4.8)	-	6 (5.7)	
Multifocal progression	26 (21.0)	4 (21.1)	22 (21.0)	
Missing	11 (8.9)	-	11 (10.5)	

* ADR n=3, OSS n=2, OTH n=2, HEP n=1

B

Variable	All patients (N=124)	cohort A (N=19)	cohort B (N=105)	p-value
Subsequent treatments (N, %)	105 (84.7)	19 (100.0))	86 (81.9)	0.04*
Distribution of subsequent treatments (n, %)				0.002*
Local treatment (LT) only	25 (23.8)	10 (52.6)	15 (17.4)	
Systemic treatment ± LT	80 (77.2)	9 (47.4)	71 (82.6)	
with ICB	46 (43.8)	4 (21.1)	42 (48.9)	0.48[a]
beyond progression	34 (32.4)	1 (5.3)	33 (38.4)	
re-induction	12 (11.4)	3 (15.8)	9 (10.5)	
without ICB	34 (32.4)	5 (26.3)	29 (33.7)	

[a] comparison of patients who received systemic treatments (with ICB vs. without ICB)